

Towards a unified theoretical model of ocean backscatter for wind speed retrieval from SAR, scatterometer, and altimeter

Craig Anderson, Trevor Macklin, Christine Gommenginger, and Meric Srokosz

Abstract. We discuss the development of a theoretical model of radar backscatter from the ocean surface which is applicable to radar altimeters, synthetic aperture radars (SAR), and scatterometers. The ultimate objective of such a model is to allow the accurate retrieval of wind speed by including all the physically important factors. Our formulation combines alternative models of the interaction between the wind and the sea surface, different descriptions of the ocean wave height spectrum and two alternative scattering theories, namely the composite-surface model and the integral equation method. The effects of swell, limited fetch, air–sea temperature difference, and rain are included. The model predictions are compared against empirical scatterometer model functions at C band, VV polarisation, where the observational behaviour has been most thoroughly studied. Published results from our model at nadir (see companion paper by Anderson et al. 2002, in this issue) agree well with the empirically observed dependence on wind speed, and the dependence on swell is consistent with recent studies. Here, results at off-nadir incidence angles show a residual discrepancy in the upwind direction which has the dimensional dependence predicted by Phillips for the radar backscatter from breaking waves. However, systematic discrepancies in the upwind to crosswind ratio indicate that the directional spread of waves is still not well understood in the theoretical modelling. Similar behaviour is also observed at Ku band, VV polarisation. The implications for the retrieval of wind speed from individual scatterometer or SAR data-takes are discussed.

Résumé. Nous discutons du développement d'un modèle théorique de rétrodiffusion radar à partir de la surface de l'océan applicable aux altimètres-radars, aux radars à synthèse d'ouverture (RSO) et aux scattéromètres. L'objectif ultime d'un tel modèle est de permettre l'extraction précise de la vitesse du vent en incluant tous les facteurs physiquement importants. Notre formulation combine des modèles alternatifs de l'interaction entre le vent et la surface de la mer, différentes descriptions du spectre de hauteur de vague océanique et deux théories alternatives de diffusion (notamment le modèle CSM (composite-surface model) et la méthode IEM (integral equation method)). Les effets de la vague, du fetch réduit, des différences de températures air–mer et de la pluie sont intégrés. Les prévisions du modèle sont comparées aux fonctions du modèle empirique de scattéromètre en bande C et en polarisation VV où le comportement des observations a été étudié plus en détail. Les résultats publiés de notre modèle au nadir (voir article d'accompagnement par Anderson et al. dans ce numéro) sont en accord avec la dépendance observée empiriquement par rapport à la vitesse de vent alors que la dépendance par rapport à la vague est cohérente avec les études récentes. Dans notre cas, les résultats pour des angles d'incidence obliques montrent une différence résiduelle dans la direction au près du vent qui présente la dépendance dimensionnelle prédite par Phillips pour la rétrodiffusion radar des vagues brisantes. Toutefois, des différences systématiques dans le ratio des vents au près par rapport aux vents de travers indiquent que l'étalement directionnel entre les vagues est encore mal connu en modélisation théorique. Un comportement semblable est aussi observé en bande Ku, en polarisation VV. On discute des implications au niveau de l'extraction de la vitesse du vent à partir d'acquisitions individuelles de données de scattérométrie ou RSO.

[Traduit par la Rédaction]

Introduction

The global information on wind and wave fields which is obtainable from spaceborne radar is important for a wide range of applications, including maritime operations, weather forecasting, and climate modelling. Useful information has been obtained from radar altimeters operating at nadir incidence and from scatterometers and synthetic-aperture radars (SAR) operating at moderate incidence angles. To date, empirical models of ocean radar backscatter have been widely used to extract quantitative information about wind fields from such data. Such models are derived from a large number of measurements and express the ocean radar backscatter as a relationship involving a few key parameters (usually wind

speed, wind direction, and incidence angle). Examples include the CMOD family of C-band models for the European remote-sensing satellite (ERS) wind scatterometer (Stoffelen and

Received 27 September 2001. Accepted 7 February 2002.

C. Anderson and T. Macklin.¹ BAE SYSTEMS Advanced Technology Centres, Great Baddow, Chelmsford, Essex CM2 8HN, United Kingdom.

C. Gommenginger and M. Srokosz. Southampton Oceanography Centre, Empress Dock, Southampton, SO14 3ZH, United Kingdom.

¹Corresponding author (e-mail: trevor.macklin@baesystems.com).

Anderson, 1993) and the altimeter algorithms that are compared by Freilich and Challenor (1994).

Theoretical models involve the calculation of the radar backscatter from realistic descriptions of the sea surface and its interaction with the wind. Hence they can address aspects neglected by present empirical models, such as the influences of swell, limited fetch, and air–sea temperature differences. Indeed, theoretical models can be used to investigate individual data-takes from a SAR or scatterometer and the overall behaviour shown by empirical models.

Here we draw on recent theoretical understanding to construct a “unified” theoretical model, that is, one with a common set of parameters applicable to SAR, scatterometer, and altimeter. A comparison between the theoretical and empirical models can thus provide insight into the physical processes that influence radar backscatter from the ocean and quantify the discrepancies that can occur when an empirical model function is applied to an individual data-take from a SAR or scatterometer.

We discuss the construction of a relevant theoretical model. The behaviour of this model at nadir incidence is discussed in a companion paper (Anderson et al., 2002). We compare the performances of the theoretical and empirical models for off-nadir incidence angles. There, we are concerned with possible systematic differences between the empirical and theoretical models, and we take account of the fact that the empirical models represent the average dependence from a large body of data. We then outline the implications of the model for the retrieval of wind speed and direction from radar sensors. There, we are interested in the possible errors that occur when the wind speed is retrieved from an individual SAR or scatterometer data-take. Lastly, we draw conclusions on the model successes and deficiencies.

Construction of a theoretical backscatter model

The formulation used in our model is discussed by Anderson et al. (2002) for the case of backscatter at nadir. Three aspects are involved, namely the description of the interaction between the wind and the sea surface, the representation of the sea surface itself, and the backscattering of incident radio waves from that surface. Hence we concentrate here on the aspects that become important when off-nadir backscatter is considered.

Interaction between the wind and the sea surface

Plant et al. (1999) and Taylor and Yelland (2001) summarize the key studies in recent years. Here, we consider the dependencies derived from three studies, namely:

- (1) the HEXOS experiment (Smith et al., 1992), which fitted the dependence of the roughness length of the sea surface, z_0 , on the wave age, c_p/u^* , where c_p is the phase speed at the peak of the wave spectrum, and u^* is the

friction velocity (defined as the square root of the ratio of wind stress to air density);

- (2) the dependence fitted by Yelland and Taylor (1996) to the neutral drag coefficient, defined as $C_D = (u^*/U_{10})^2$, where U_{10} is the wind speed at 10 m altitude; and
- (3) an explicit dependence on significant wave height, H_s , using the description of z_0/H_s as a power-law dependence on H_s/L_p fitted by Taylor and Yelland (2001), where L_p is the peak wavelength in the wave height spectrum.

The expressions for models 1–3 are given by Equations (2)–(4), respectively, in Anderson et al. (2002). These relationships, combined with the model for the wind speed at height z ,

$$U(z) = \frac{u^*}{0.4} \left[\ln \left(\frac{z}{z_0} \right) - \Psi \right] \quad (1)$$

where Ψ is a stability function that describes the effects of differences between the air and sea temperatures, allow the friction velocity to be calculated. Here we use the formulation of Ψ given by Equations (13) and (12) in Geernaert et al. (1987) for stable cases (air warmer) and unstable cases (sea warmer), respectively.

Note that there is a discontinuity when model 3 is applied to combined wind seas and swell, because L_p will shift from the peak of the wind sea to the peak of the swell if the swell height increases at fixed wind speed. In practice, however, this discontinuity does not have a significant impact on our results.

Also note that for fully developed seas with neutral stability and no swell, all these models give similar relationships between the friction velocity and U_{10} (Anderson et al., 2002, Figure 2).

Description of the sea surface

A description of the sea surface is required over a broad range of scales, from centimetre scales commensurate with the radar wavelength up to scales of several hundred metres to represent ocean swell. This has been a key area of research for many years and there is still a considerable lack of consensus among alternative models. In recent years, a number of attempts have been made to develop realistic descriptions of the ocean wave height spectra of wind seas, without using radar data as a constraint. (Otherwise this would lead to a circular argument in the testing of the combined surface and backscatter model against radar data.) Apel (1994), Elfouhaily et al. (1997), and Lemaire et al. (1999) have developed models in this way. The Apel model gives the two-dimensional surface height spectrum as a function of wind speed and direction but only represents fully developed wind seas. These are defined by Pierson (1991) as being solely a function of wind speed, provided that the distance over which the wind has blown is larger than a certain distance and the duration of the wind is greater than a certain time. The other two models also include

the effects of fetch and friction velocity, and they are the models discussed here.

The spectrum of Elfouhaily et al. (1997), in particular, is consistent with a wide set of observational data, is analytically continuous, and has no aphysically tuned parameters. The Lemaire et al. (1999) spectrum requires a free parameter to be set, namely the significant slope, which is defined as the root mean square (rms) surface height divided by the wavelength of the peak in the spectrum. Lemaire et al. estimate this by fitting to radar data. Apart from the circular argument referred to in the previous paragraph, the fitting procedure may be affected by the presence of swell. Alternatively, as shown in **Figure 1**, we can set the significant slope by matching the mean square slope of the Lemaire et al. spectrum as a function of U_{10} with the empirical model of Cox and Munk (1954). This gives a best-fit significant slope of around 0.60%.

Note that all the spectra considered here have been constructed by their authors so that they die off faster than k^{-4} at high wavenumbers which results in a convergent result for the calculation of the mean square slope (see the discussion in Glazman, 1990; 1991).

Our model allows the inclusion of a two-dimensional Gaussian spectrum in wavenumber space to represent swell. It also has the option to incorporate perturbations in the wave spectrum due to rain using the model of Bliven et al. (1997).

The directional spread of wave energy has an important influence on the predicted backscatter at off-nadir incidence angles. However, this quantity is not well determined experimentally, and so previous authors have resorted to assumed functional forms. Elfouhaily et al. (1997) give an overview of these and describe a formulation aimed at unifying the behaviour at long and short waves in a consistent manner.

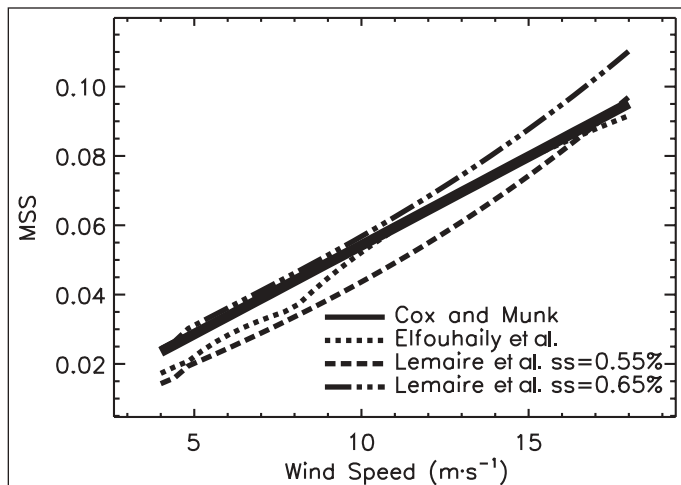


Figure 1. Mean square slope (MSS) of Elfouhaily et al. (1997) and Lemaire et al. (1999) wave spectra compared with the empirical dependence on wind speed from Cox and Munk (1954). ss, value of the significant slope in the Lemaire et al. spectrum.

Description of backscatter from the sea surface

The scattering model must include the contributions from surface scales commensurate with the radar wavelength and from longer scales. The relative contribution from these scales depends on the incidence angle and affects the dependence on radar polarisation. We consider two scattering models that provide a realistic but relatively simple computational solution and have been widely applied to studies of radar backscatter from the ocean: (1) the composite-surface model, which considers the surface to consist of patches of small-scale roughness tilted and modulated by longer wavelengths (Valenzuela, 1978); and (2) the integral equation method (IEM), which, in theory, treats all wavelengths in a consistent manner (Chen et al., 1992).

The split into two scales is an artifice of the composite-surface model. The calculated cross section is insensitive to the wavenumber of this split, provided that wavenumber is about 0.3 times the radar wavenumber (see the discussion in Anderson et al., 2002).

In practice, our implementation of the IEM requires two dividing wavenumbers to be set for its numerical implementation. One is a physically based wavenumber chosen to mark out the wavelengths that contribute to specular scattering when the incidence angle tends towards zero, and the other is a computationally based wavenumber related to the grid size used in the Fourier transform. The values used here are 1.50 and 0.05 times the radar wavenumber, respectively. With these values, the two-scale and IEM models agree to within about 0.1 dB in C band, VV polarisation (C-VV), for incidence angles out to 50° and wind speeds up to 18 m·s⁻¹. Hence only results using the composite-surface model will be presented here. (Note that Voronovich and Zavorotny (2001) use the small-slope approximation to calculate the scattering; this is a more rigorous formulation than the IEM, but it gives very similar results in the VV polarisation considered here.)

Here we concentrate on results at VV polarisation because the empirical model function is particularly well established at C band, and results at Ku band are also available for comparison. The choice of scattering model is a more significant issue for HH polarisation because of the greater influence of factors such as wave breaking (e.g., Jessup et al., 1990; Voronovich and Zavorotny, 2001). Note that the model used here neglects the possible contribution of scattering from breaking or near-breaking waves. We return to this issue later in the paper.

Off-nadir behaviour

Wind vector information on a global scale is routinely retrieved from off-nadir measurements of backscatter provided by radar scatterometers. Images produced by SAR systems have also been used to examine the wind field in local areas. As with the nadir case, empirical models of ocean radar backscatter are widely used to retrieve the wind information. These models express the ocean backscatter as a function of the

wind speed and the azimuthal angle between the wind and radar look directions. Three important characteristics of these models are the backscatter in the upwind direction (i.e., where the wind direction and the radar look direction coincide), the upwind to crosswind backscatter ratio, and the upwind to downwind backscatter ratio. The last of these is sensitive to hydrodynamic modulations (e.g., Plant, 1986) and is not discussed here.

In this section, we concentrate on the behaviour at C band, VV polarisation (C-VV) and include results from Ku band, VV polarisation where they add additional information to the interpretation. The comparison of empirical and theoretical models of ocean backscatter at C and Ku bands is also discussed by Voronovich and Zavorotny (2001), but only for the case of fully developed wind seas in the absence of swell. Our results are in close agreement with theirs in this limit. However, here we evaluate additional factors, including the influences of swell, wave age, and the air-sea interaction.

Upwind behaviour at C band, VV polarisation

A variety of empirical models exists for C-VV backscatter, including CMOD4 (Stoffelen and Anderson, 1993), CMOD3 (Long, 1995), and IFR2 (Quilfen and Bentamy, 1994). These models are well developed; Stoffelen and Anderson (1997) show that CMOD4 fits measured backscatter from the ERS wind scatterometer to within 0.2 dB, statistically. **Figure 2** compares the upwind backscatter predicted by several empirical models. These agree to within 1 dB over much of the range of wind speeds shown, with some larger disagreements at low wind speeds and high incidence angles. Although these empirical models are well developed and widely used, they do not include factors such as swell or air-sea temperature difference which can affect the ocean backscatter.

Figure 3 compares the behaviour of the theoretical model described earlier in the paper with the IFR2 empirical model. Differences between the theoretical and empirical models may be caused by a variety of factors, including the presence of

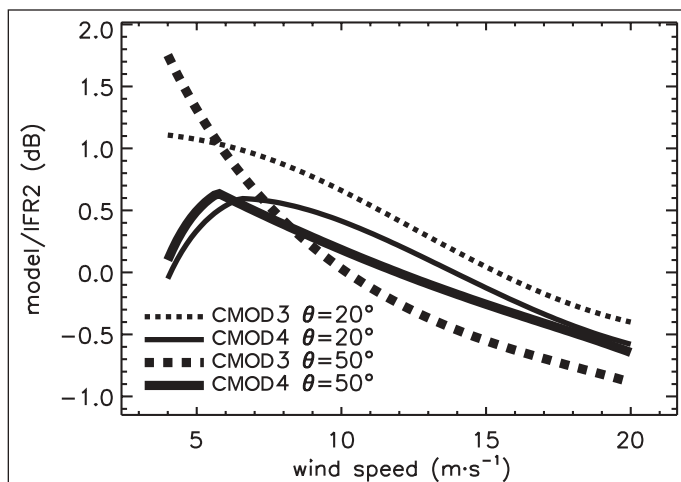


Figure 2. Comparison of upwind C-VV backscatter from three empirical models. Values from CMOD3 and CMOD4 are plotted relative to IFR2 for incidence angles $\theta = 20^\circ$ and 50° .

swell and the influence of wave breaking. Here, **Figure 3a** shows that the greatest difference with the Elfouhaily et al. (1997) spectrum is about 3 dB at high wind speeds and 50° incidence. The effects of the HEXOS, Yelland and Taylor (1996), and Taylor and Yelland (2001) models for the air-sea interaction (labelled hex, y&t, and t&y) are also shown and have only a minor effect at larger wind speeds. However, the HEXOS model at higher wind speeds and the Taylor and Yelland model at lower wind speeds give slightly better agreement. Note that the Elfouhaily et al. spectrum displays a discontinuity at around $7 \text{ m}\cdot\text{s}^{-1}$ as it moves between two different regimes.

For the Lemaire et al. (1999) spectrum with the HEXOS model (**Figure 3b**), we find that the value of the significant slope has a significant effect on the comparison at 20° incidence and very little effect on the backscatter at 50° . For a significant slope of 0.6%, chosen in the previous section by

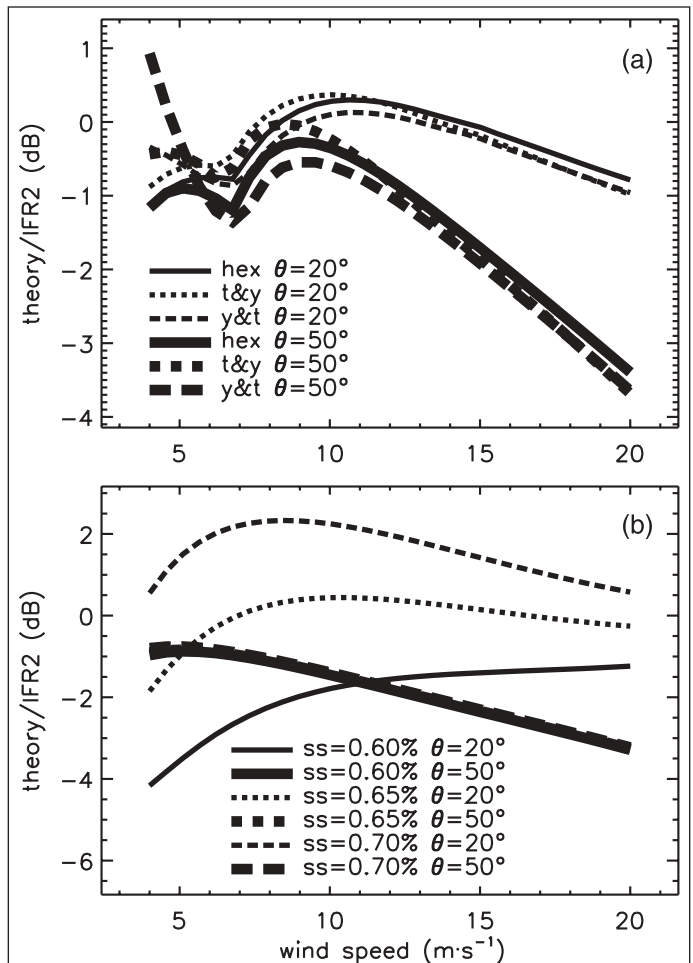


Figure 3. Comparison of C-VV backscatter from empirical and theoretical models with (a) the Elfouhaily et al. (1997) spectrum and HEXOS (hex), Taylor and Yelland (2001) (t&y), and Yelland and Taylor (1996) (y&t) descriptions of the air-sea interaction; and (b) the Lemaire et al. (1999) spectrum with the HEXOS description of the air-sea interaction and different significant slopes (ss). Results are shown for incidence angles $\theta = 20^\circ$ and 50° in the upwind direction.

comparison with the Cox and Munk (1954) model, the Lemaire et al. spectrum produces a greater discrepancy than that of Elfouhaily et al. (1997). The significant slope could be adjusted to reduce the discrepancy. As discussed earlier, however, tuning the spectrum in this manner is undesirable on the grounds that the empirical model may have been affected by environmental conditions and the inaccuracy in the theoretical model may be due to the modelling of the scattering or air–sea interaction rather than the ocean spectrum.

We now examine whether the inclusion of additional environmental effects may reduce the discrepancy between the empirical and theoretical models in **Figure 3**, in particular the discrepancies greater than 1 dB at 50° incidence. The modelling allows us to assess the effects of wave age, rain, and the air–sea temperature difference, but these are not expected to be the most significant factors when data from all over the world are averaged to produce an empirical model function. For example, Quartly et al. (1999) infer that the probability of rain is only around 5% over the open ocean. However, these factors are important in considering the accuracy of the wind speeds retrieved from *individual* SAR or scatterometer data-takes, and so they are considered later in the paper. Here, the most relevant effects that could produce *systematic* biases between empirical and theoretical models are the influences of swell and wave breaking, as these could influence data obtained anywhere. Hence we consider these two effects first.

Swell

Measurements of radar backscatter have shown some dependence on the presence of large swell waves under light winds (Nghiem et al., 1995). In other cases, there is no direct correlation with swell properties but there is an overall deviation with backscatter model functions on the order of 1 dB which could be attributable to the effects of surface conditions (Nghiem et al., 1997). Since these trends are consistent with earlier theoretical predictions (Durden and Vesecky, 1985), we need to consider the predictions of the impact of swell in our own model.

Here a range-travelling Gaussian swell of mean wavelength 200 m (to represent a typical deep-ocean value), with a standard deviation of 10° in angle and an equivalent spread in wavelength, was added to the 14 m·s⁻¹ wind-sea spectrum to simulate ocean swell. As discussed earlier, the swell can affect the backscatter through its effects on long-wave statistics and friction velocity. The direction of the swell relative to the wind spectrum is also significant. **Figure 4** shows that, with the combined wind-sea and swell spectrum, the backscatter at both 20° and 50° increases with an increase in the rms swell height. The rates of increase with the increase in rms swell height are slightly greater at C band than at Ku band. Results for the Lemaire et al. (1999) spectrum are similar. Note that, as discussed in earlier in the paper, there is a discontinuity in the results caused by the peak in the spectrum moving from the wind sea to the swell.

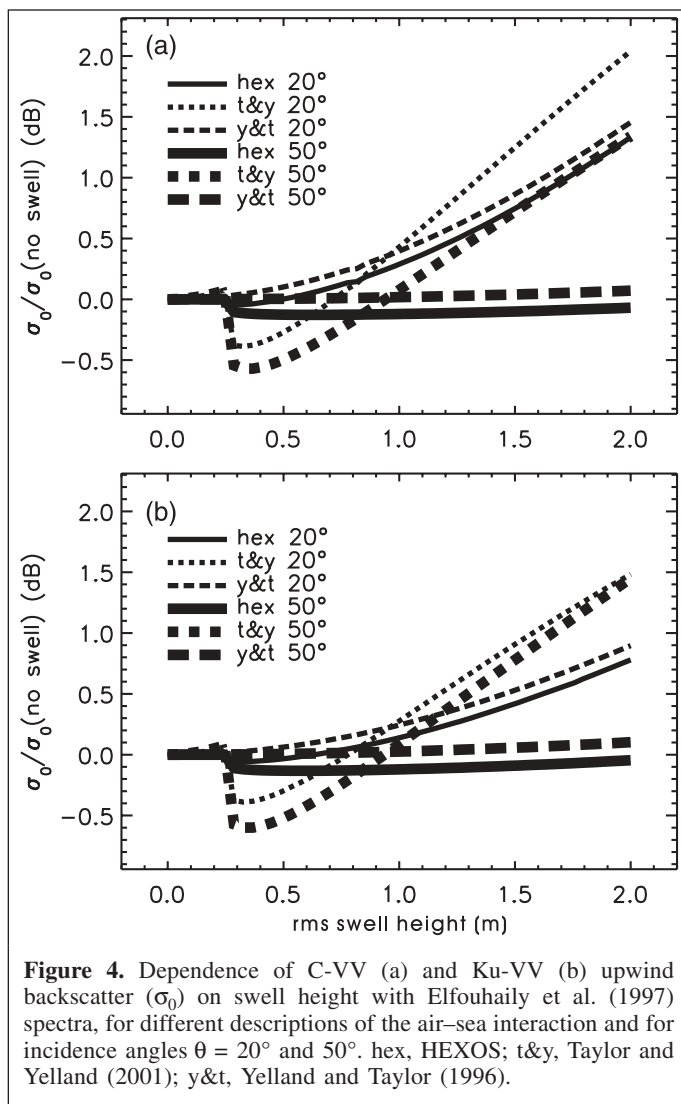


Figure 4. Dependence of C-VV (a) and Ku-VV (b) upwind backscatter (σ_0) on swell height with Elfouhaily et al. (1997) spectra, for different descriptions of the air–sea interaction and for incidence angles $\theta = 20^\circ$ and 50° . hex, HEXOS; t&y, Taylor and Yelland (2001); y&t, Yelland and Taylor (1996).

Wave breaking

Models of the wave spectrum based on observational data (including the Elfouhaily et al. (1997) and Lemaire et al. (1999) spectra) implicitly incorporate some aspects of wave breaking. However, there are various definitions of what constitutes wave breaking: it consists of intermittent events both spatially and temporally and has a different angular behaviour from that of the wind sea. These facts make it difficult to formulate a model for the effects of wave breaking on the statistics of the sea surface elevation and slopes. Available models include that of Belcher and Vassilicos (1997), who derive a spectrum explicitly containing the effects of breaking waves, although only for the gravity-controlled equilibrium part of the spectrum.

A simpler approach is adopted by Phillips (1988), who uses dimensional analysis to model the contribution of breaking to the backscatter and finds that it varies as the cube of the friction velocity u^* . **Figure 5** shows the backscatter difference between the empirical and theoretical models over the wind speed range 4–20 m·s⁻¹ (which, with the HEXOS model, corresponds to a

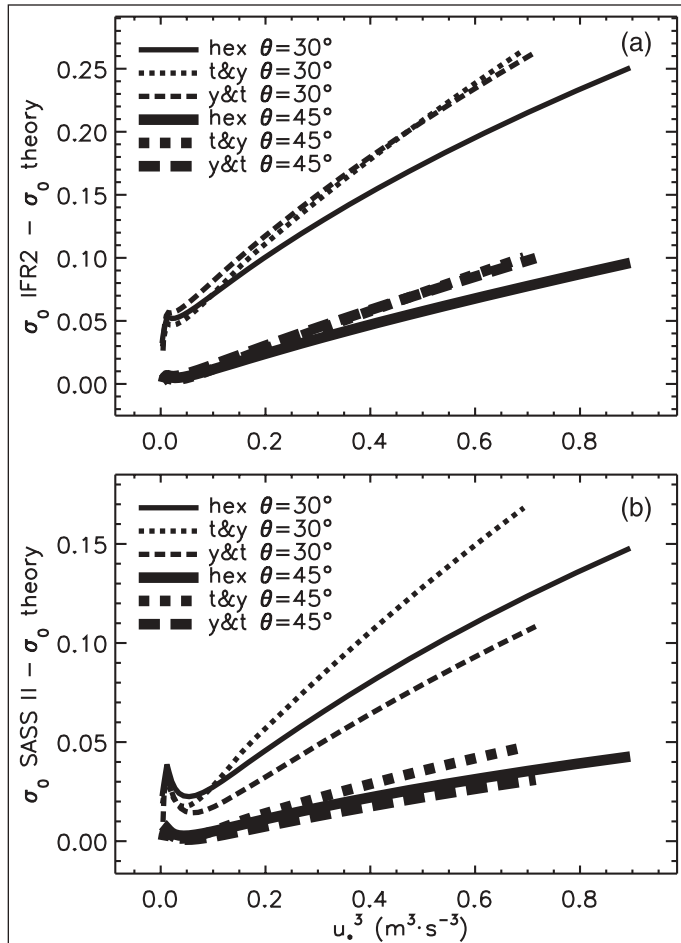


Figure 5. Residual backscatter for C-VV (a) and Ku-VV (b) in the upwind direction as a function of the cube of the friction velocity u_*^3 . The plots show the difference in the actual cross sections (not in dB) between theoretical predictions using the Elfouhaily et al. (1997) wind spectrum and empirical models (IFR2 for C-VV and SASS II for Ku-VV). hex, HEXOS; t&y, Taylor and Yelland (2001); y&t, Yelland and Taylor (1996).

range in u_*^3 of 0.15–0.96 $\text{m}^3 \cdot \text{s}^{-3}$). The empirical models used here are the IFR2 model (Quilfen and Bentamy, 1994) at C band and the SASS II model function (Wentz et al., 1984) at Ku band. At moderate incidence angles for VV polarisation in both C band and Ku band, we find that the backscatter difference follows the power-law dependence proposed by Phillips over a wide range. Note that it is appropriate to test the Phillips model at moderate incidence angles because his analysis is derived for this case, as it neglects the contribution from specular scattering in the composite-surface model. Also, the results at Ku band (Figure 5b) are consistent with the measurements of Jessup et al. (1990) at this frequency in the North Sea. Jessup et al. also found a cubic dependence on u_*^3 , and their estimate that 5–10% of the Ku-VV backscatter at 25–45° incidence is associated with steep or breaking waves agrees well with our results.

Effects of wave age, rain, and air–sea temperature difference

We now consider additional factors that might influence the estimation of wind speed from individual SAR or scatterometer data-takes. The effects of wave age, rain, and the air–sea temperature difference are discussed in turn.

Wave age

Figure 6a shows the typical effect of changing the wave-age parameter in the Elfouhaily et al. (1997) omnidirectional spectrum. As the wave age increases the longer wavelengths contribute more to the surface roughness. Within the theoretical model this affects the backscatter in two ways: first, it changes the long-wave slope statistics; and second, it may alter the friction velocity (depending on the air–sea interaction model, as reviewed earlier in the paper), which then affects the short-wavelength part of the wind-sea spectrum. Figures 6b and 6c show the effect on the backscatter of varying the wave-age parameter in the Elfouhaily et al. spectrum with a wind speed of 14 $\text{m} \cdot \text{s}^{-1}$. The results are shown relative to the backscatter produced with a wave age of 1.2, which is the maximum permitted by the spectrum. As the wave age decreases the backscatter at 50° increases and that at 20° decreases. The dependences at C band are stronger than those at Ku band. Results using the Lemaire et al. (1999) spectrum are similar, but with a larger change in the backscatter at 20°.

Rain

Melsheimer et al. (1998) summarize previous studies of the effects of rain on SAR images and interpret multifrequency, polarimetric data from the Shuttle Imaging Radar SIR-C/X-SAR. They argue that the dominant factors which influence the microwave backscatter at centimetre wavelengths are the scattering and attenuation by rain and ice particles in the atmosphere and the modification of the sea surface by the impact of raindrops. For the latter process, they use the model spectrum derived by Bliven et al. (1997) for the effects of rain-induced “ring waves” on the ocean surface.

Figure 7 shows the effects of adding the Bliven et al. (1997) spectrum to the 14 $\text{m} \cdot \text{s}^{-1}$ wind-sea spectrum. This figure predicts that the C-VV backscatter will be affected more strongly by the rain at 50° incidence than at 20° incidence, but the increase and the dependence on incidence angle are less strong at Ku band.

To evaluate the attenuation, we follow the model of Goldhirsh and Rowland (1982), who represent the attenuation coefficient k (in dB/km) as

$$k = aR^b \quad (2)$$

where R is the rain rate in mm/h, and a and b are empirically fitted parameters that depend on the radar frequency and the drop-size distribution.

Olsen et al. (1978) quote values in the range $a = 0.00112$ to 0.00241 and $b = 0.896$ to 1.288 at 5 GHz, depending on the

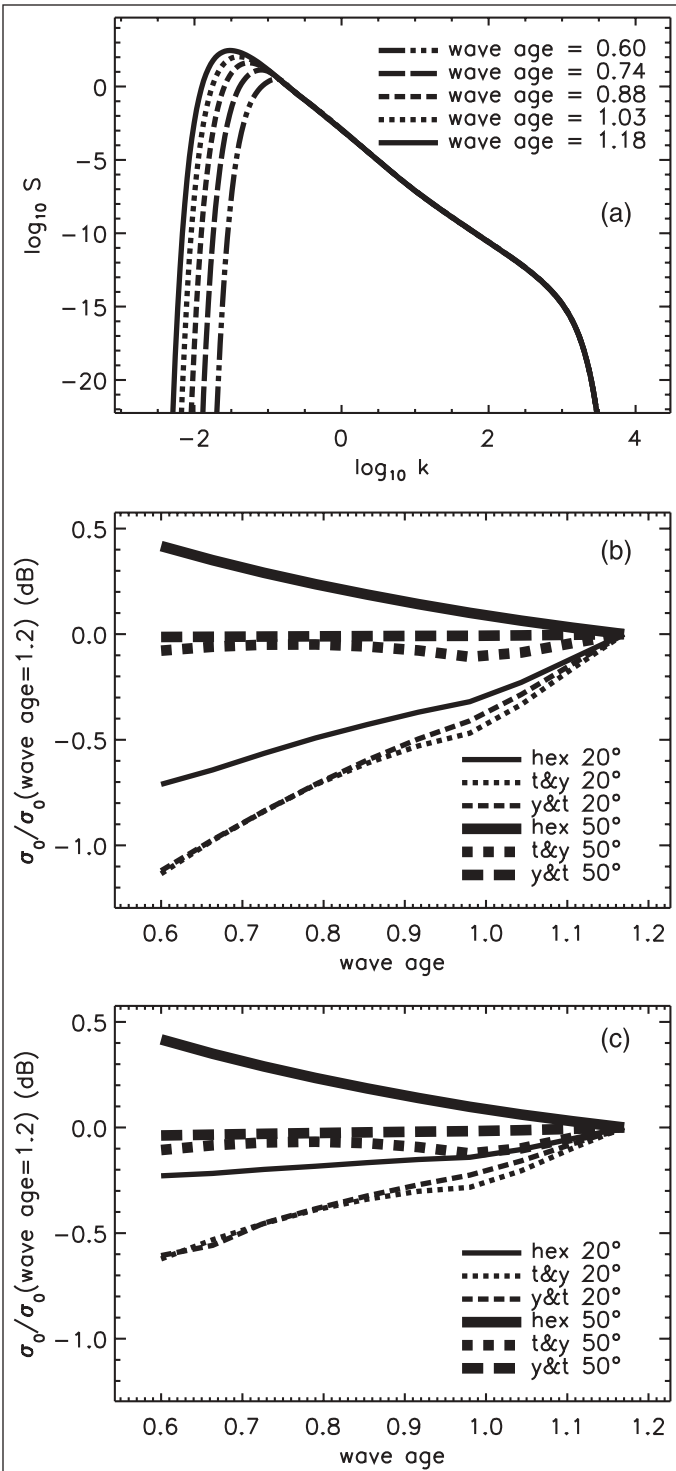


Figure 6. Effect of wave age on the Elfouhaily et al. (1997) wave spectrum (a) and on the predicted behaviour of the upwind ocean backscatter for C-VV (b) and Ku-VV (c). The plots in (b) and (c) show the dependences for the air-sea interaction models and incidence angles as in Figure 4. hex, HEXOS; ss, significant slope; t&y, Taylor and Yelland (2001); y&t, Yelland and Taylor (1996).

assumed drop-size distribution, for a rain temperature of 0°C. Here we use their median values of $a = 0.00194$ and $b = 1.113$.

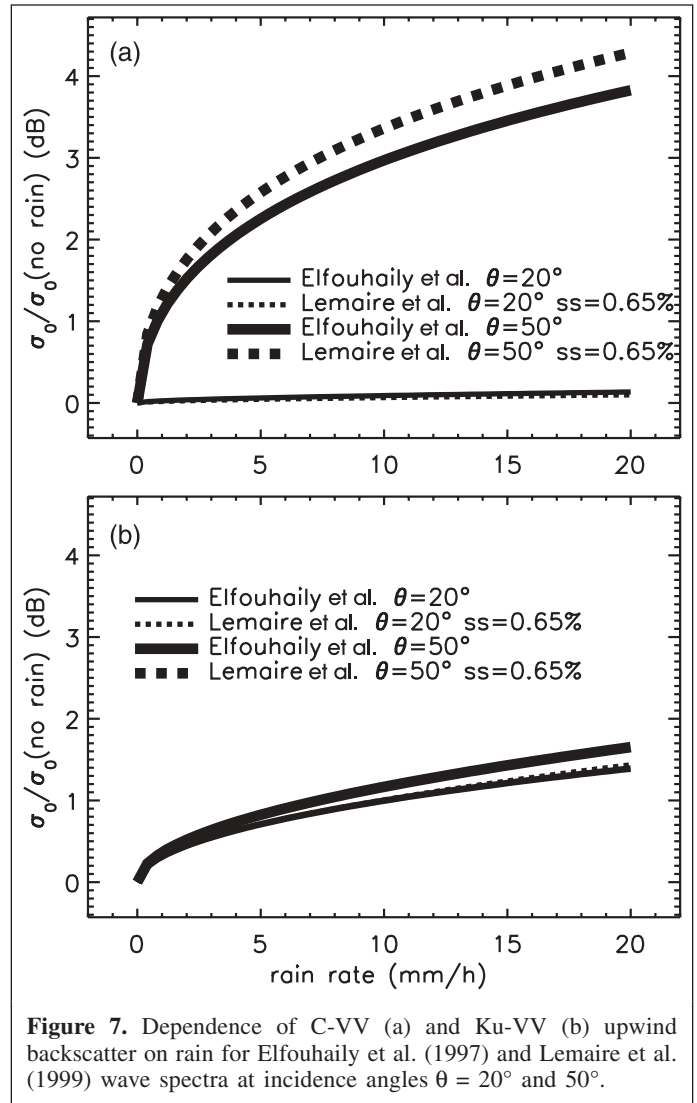


Figure 7. Dependence of C-VV (a) and Ku-VV (b) upwind backscatter on rain for Elfouhaily et al. (1997) and Lemaire et al. (1999) wave spectra at incidence angles $\theta = 20^\circ$ and 50° .

Assuming uniform rain through a typical rain cell of height 5 km, the total attenuation in the two-way path at nadir is 0.25 dB at a rain rate of 10 mm/h and 0.85 dB at a rain rate of 30 mm/h. Repeating the calculation for 15 GHz, the corresponding median values are $a = 0.03680$ and $b = 1.118$, giving two-way attenuations of 4.8 and 16 dB for rain rates of 10 and 30 mm/h, respectively. Hence, the attenuation in rain is much greater at Ku band than at C band. These values scale with incidence angle θ as $1/\cos \theta$, assuming that the total propagation path remains within the rain cell. On this assumption, the attenuation in dB at 50° incidence is 1.9 dB more than that at nadir; this is an overestimate of the attenuation at off-nadir incidence if the rain cell size is inversely correlated with the rain rate, as found by Goldhirsh (1983).

Air-sea temperature difference

The air and sea temperatures appear implicitly in Equation (1) and affect the calculation of the friction velocity. This is the standard formulation of the influence of air-sea

temperature difference which is used in many previous studies, including Keller et al. (1989), and in the demonstration of Wu (1991) that the results of Keller et al. are consistent with the behaviour in optical measurements of the mean-squared slope. Equation (1) implies that the influence of the air-sea temperature is strongest at low wind speeds, and this aspect is discussed further by Colton et al. (1995) and Plant et al. (1999).

Table 1 shows the frequency of occurrence of a range of temperature differences, as recorded by three ocean weather buoys, namely 42000 (latitude 25.89°N, longitude 93.57°W), 44014 (latitude 36.58°N, longitude 74.83°W), and 51026 (latitude 21.4°N, longitude 147.0°W). The measurements were taken in 1996 and were coincident to within half an hour and 25 km with measurements from the ERS scatterometer.

Table 1 indicates the air and sea temperatures typically differ by less than 2°C. Taking a sea temperature of 10°C, **Figure 8** shows the effect of a 2°C variation in air temperature on C-VV backscatter. These results suggest that the model's greatest sensitivity is at low wind speeds at higher incidence angles.

Upwind to crosswind ratio

The upwind to crosswind backscatter ratio is an important characteristic of ocean backscatter. **Figure 9** compares this ratio for the three C-VV empirical backscatter models, namely CMOD3, CMOD4, and IFR2. These models generally agree to within 1 dB over much of the range of wind speeds shown, although there are some larger disagreements at larger incidence angles and high wind speeds.

Figure 10 shows the difference (in dB) between the upwind to downwind backscatter ratios from the theoretical model and those from the IFR2 empirical model. The model results with

Table 1. Frequency of occurrence of sea-air temperature differences ($T_S - T_A$) for three ocean weather buoys.

$T_S - T_A$ (°C)	Frequency of occurrence		
	Buoy 42002	Buoy 44014	Buoy 51026
-7	0	2	0
-6	0	23	0
-5	0	97	0
-4	0	321	0
-3	0	664	0
-2	37	1127	0
-1	1489	1805	318
0	3006	1347	4444
1	1016	725	1536
2	440	258	580
3	244	171	280
4	171	109	39
5	91	114	2
6	63	111	0
7	57	78	0
8	119	21	0
9	87	1	0
10	11	0	0
Total	6831	6974	7203

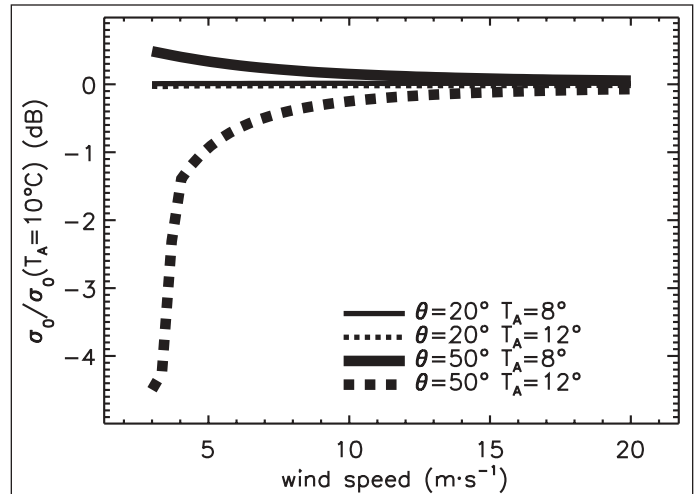


Figure 8. Dependence of C-VV upwind backscatter on air temperature (T_A , in °C) for a sea temperature (T_S) of 10°C at incidence angles $\theta = 20^\circ$ and 50° . ss, significant slope.

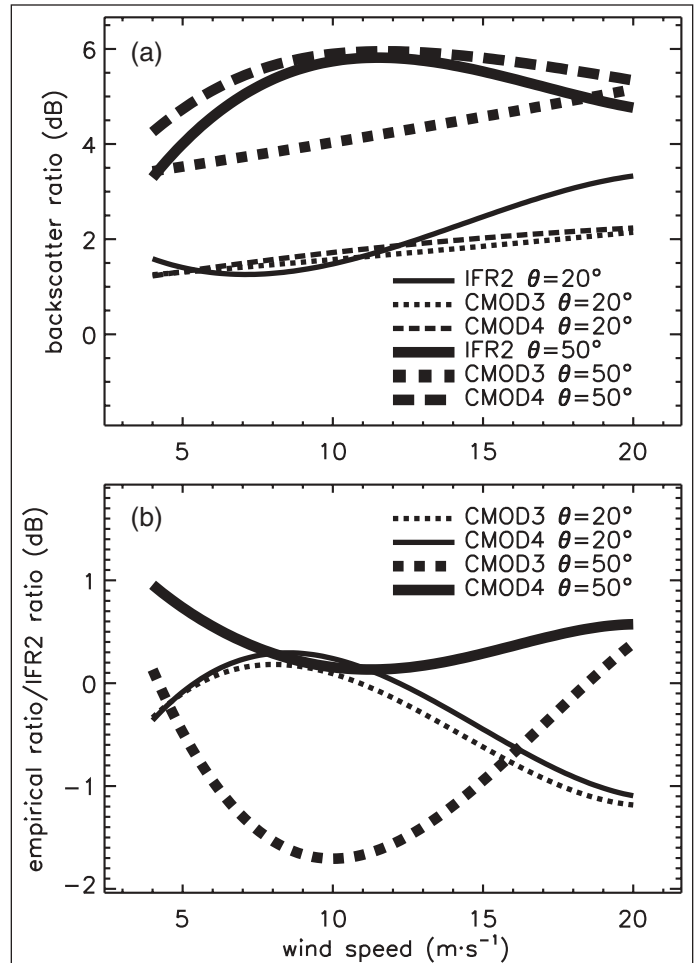
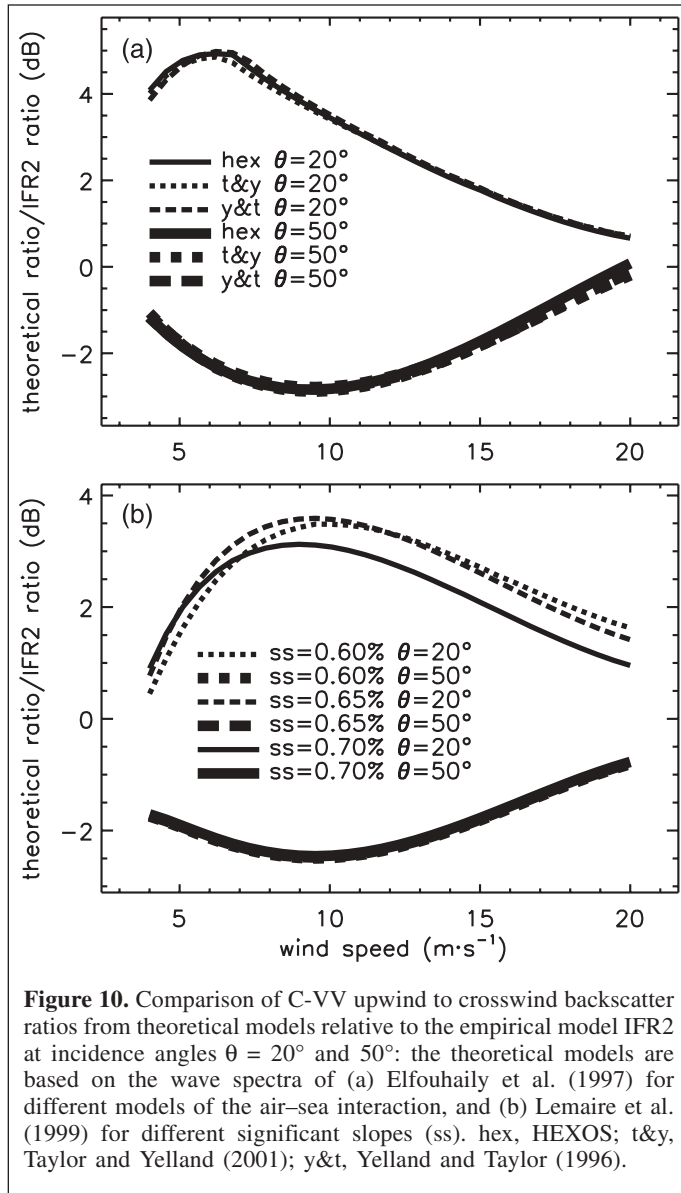


Figure 9. Comparison of upwind to crosswind backscatter ratios from C-VV empirical models at incidence angles $\theta = 20^\circ$ and 50° : (a) absolute values of the upwind to crosswind ratio, and (b) upwind to crosswind ratios relative to the ratio for the empirical model IFR2.

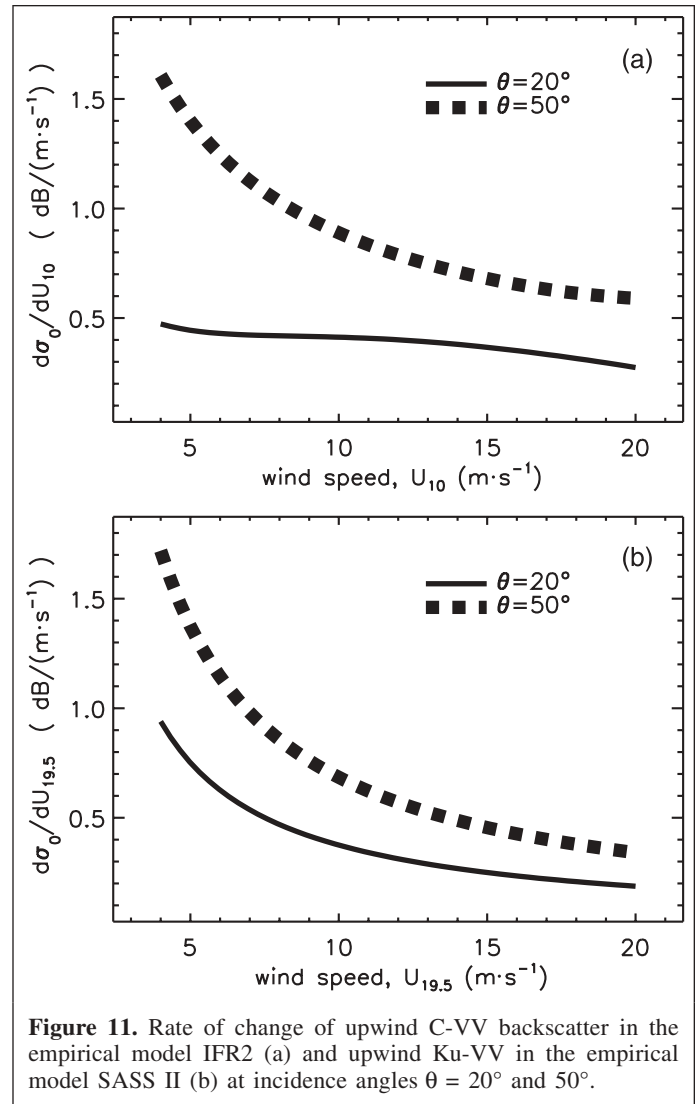
Canadian Journal of Remote Sensing Downloaded from pubs.casi.ca by IPREMER BIBLIOTHEQUE LA PEROUSE on 03/23/13 For personal use only.



both the Elfouhaily et al. (1997) and Lemaire et al. (1999) spectra show large discrepancies with the empirical model. Voronovich and Zavorotny (2001) obtain similar conclusions at both C band and Ku band. We note that the upwind to crosswind ratio is strongly affected by the directional spread of wave energy in the ocean spectra and that this quantity is not yet well determined experimentally. A description for the directional spread which unifies the behaviour at long and short waves in a consistent manner remains an important area of investigation.

Implications for wind speed retrieval

It is important to understand the implications of the theoretical model for the retrieval of wind speeds from radar data. An error of $1 \text{ m}\cdot\text{s}^{-1}$ in retrieved wind speed may seem small, as it is comparable to the error in individual in situ



measurements. However, a systematic error of this magnitude would be a significant bias in statistical analyses of wind and wave climate. Such errors have already been found; for example, Rufenach et al. (1998) propose using different empirical models in different regions of the Pacific which are subject to different fetch and swell regimes.

Figure 11 shows the predicted rate of change of the upwind backscatter with the wind speed for the IFR2 (Quilfen and Bentamy, 1994) and SASS II (Wentz et al., 1984) empirical backscatter models. These results imply that a change of wind speed of $1 \text{ m}\cdot\text{s}^{-1}$ corresponds to a change in backscatter of around 0.5 dB at 20° and around 1.0 dB at 50° . Hence any phenomena which change the backscatter by around 0.5 dB at 20° or 1 dB at 50° could potentially cause an approximately $1 \text{ m}\cdot\text{s}^{-1}$ retrieval error in the wind speed. (Note, however, that such changes in backscatter cause slightly lower errors in the retrieved wind speed at Ku band than at C band according to **Figure 11**.)

The theoretical model described earlier in the paper indicates that the environmental effects which may cause such errors on

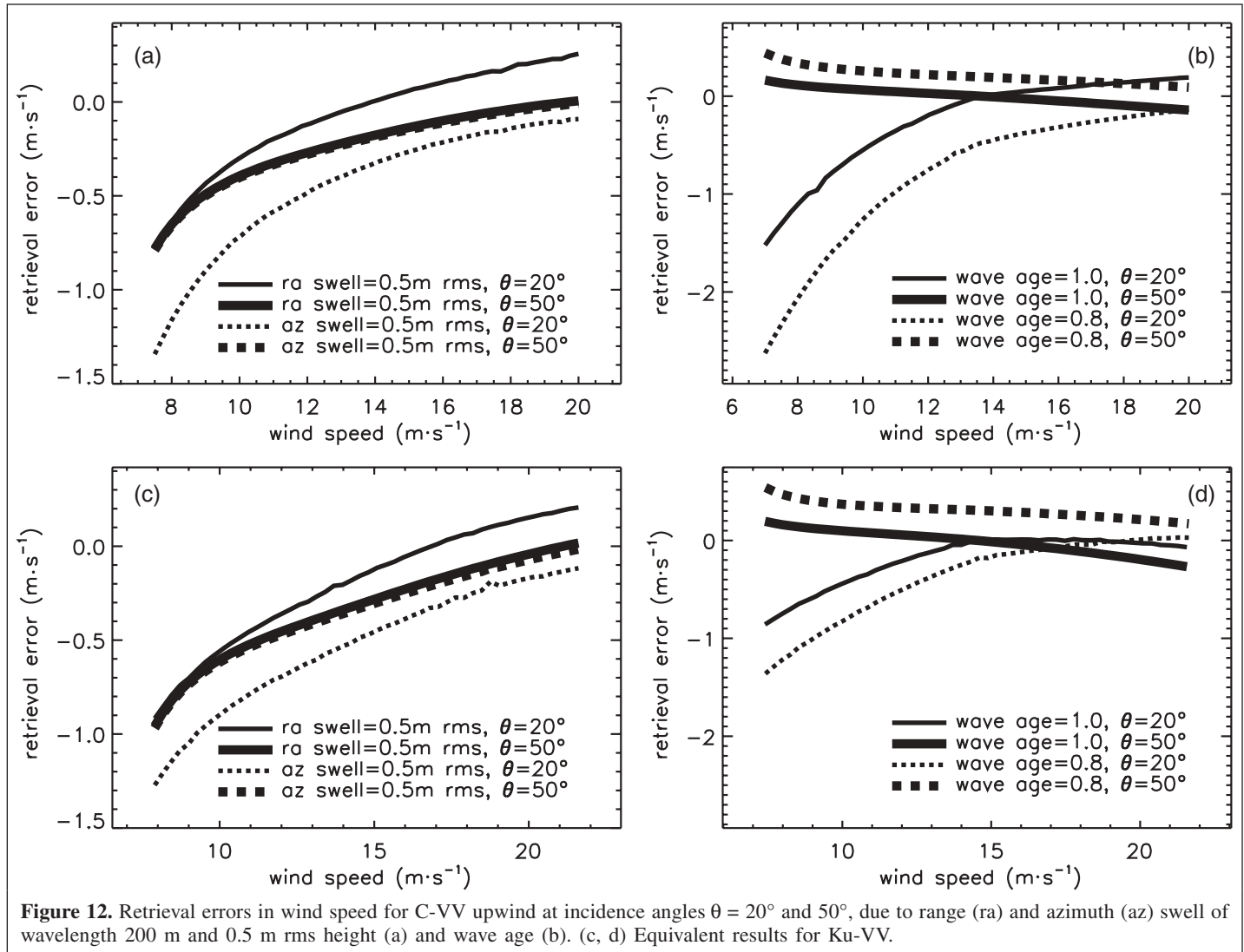


Figure 12. Retrieval errors in wind speed for C-VV upwind at incidence angles $\theta = 20^\circ$ and 50° , due to range (ra) and azimuth (az) swell of wavelength 200 m and 0.5 m rms height (a) and wave age (b). (c, d) Equivalent results for Ku-VV.

individual data-takes are (1) swell at low incidence angles; (2) rain at high incidence angles; (3) an air–sea temperature difference at low wind speeds, particularly when the air is warmer (stable conditions); and (4) a possible contribution from wave breaking.

A more detailed method of quantifying the wind retrieval error is to examine the behaviour of a retrieval algorithm in response to the simulated backscatter provided by the theoretical model. Examples of this approach are shown in **Figures 12** and **13**. Here we assume that the wind direction is known and we use the IFR2 or SASS II empirical model to retrieve the wind speed with and without a perturbation to the backscatter. The magnitude of the perturbation is provided by the theoretical model with either range and azimuthal swell, varying wave ages or air temperature. (Note that we do not have a model of wave breaking to perturb the theoretical model in this way. However, the conclusion given earlier, namely that any phenomenon which changes the backscatter by around 0.5 dB at 20° or 1 dB at 50° could potentially cause an approximately $1 \text{ m}\cdot\text{s}^{-1}$ retrieval error in the wind speed, applies to the contribution from breaking waves. Hence this conclusion

can be used to estimate the effect on wind speed retrievals if the contribution of breaking waves to the mean cross section is already known, for example from measurements such as those of Jessup et al. (1990).)

These results predict that swell and wave age can cause a significant error (more than $1 \text{ m}\cdot\text{s}^{-1}$) in wind speed retrieval at lower incidence angles for C band, and the greatest error from these factors at Ku band is about $1 \text{ m}\cdot\text{s}^{-1}$. The neglect of an air–sea temperature difference may cause a significant error at lower wind speeds and high incidence angles for both C band and Ku band.

Conclusions

A theoretical model for the radar backscatter from the ocean, applicable to both nadir and off-nadir incidence angles, has been discussed. The model combines representations of the interaction between the wind and the sea surface, the sea surface itself, and the interaction of radio waves with that surface.

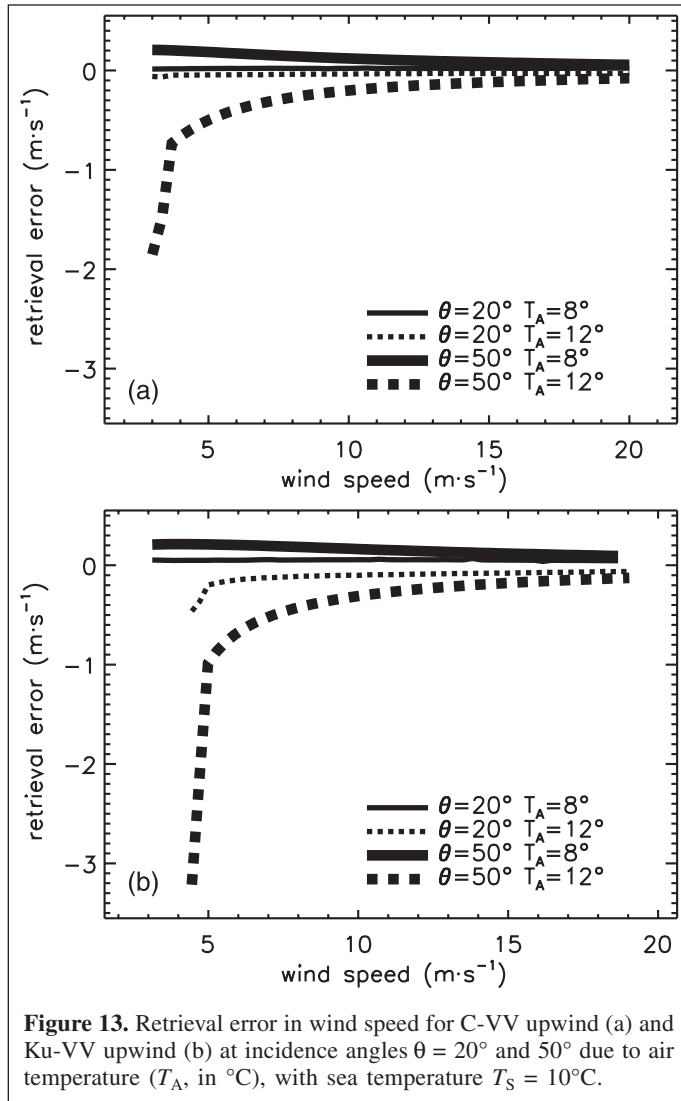


Figure 13. Retrieval error in wind speed for C-VV upwind (a) and Ku-VV upwind (b) at incidence angles $\theta = 20^\circ$ and 50° due to air temperature (T_A , in $^\circ\text{C}$), with sea temperature $T_S = 10^\circ\text{C}$.

A comparison for nadir backscatter between the theoretical model and the empirical model of Gommenginger et al. (2002) is discussed in Anderson et al. (2002). As the empirical model is not calibrated on an absolute scale, that comparison focuses on whether the theoretical model can reproduce similar rates of change of backscatter with key oceanographic parameters. The dependence on swell rms height was found to be strongly influenced by the assumed interaction between the wind and the sea surface, and the dependence on wave age was strongly influenced by the assumed wind-sea spectrum. The closest agreement was obtained by using the wind-sea spectrum description of Elfouhaily et al. (1997) with the HEXOS (Smith et al., 1992) or Yelland and Taylor (1996) descriptions of the interaction between the wind and the sea surface.

In this paper we have examined the behaviour of the physically based model in the off-nadir regime. The Elfouhaily et al. (1997) spectrum with either the HEXOS (Smith et al., 1992) or the Taylor and Yelland (2001) model for air-sea interaction provide a good fit in the upwind direction to scatterometer model functions developed at C band, VV

polarisation. However, a discrepancy that increases with increasing wind speed is found. A variety of environmental factors have been evaluated to determine if their inclusion in the theoretical model would reduce or remove this discrepancy. The discrepancy varies with the cube of the friction velocity as predicted by Phillips' (1988) dimensional analysis of the backscatter from breaking waves, and the results are also consistent with the measurements of Jessup et al. (1990).

The theoretically predicted upwind to crosswind ratio does not fit well with the empirical model, implying that the directional dependence of the wind-sea spectrum is not well understood. These conclusions are not affected by the choice of scattering model considered here, namely the IEM or composite-surface model.

Voronovich and Zavorotny (2001) have recently compared empirical and theoretical models of backscatter. However, they consider the discrepancies between the two to be due solely to the effect of steep breaking waves and then proceed to modify the probability density function of large sea surface slopes to bring about a better agreement. This runs counter to our modelling approach, outlined earlier in the paper, that aims to use a description of the sea surface which is completely independent of radar data. Our work has also considered a much wider range of factors than that of Voronovich and Zavorotny, including the effects of wave age, swell, air-sea interaction, and different models for the ocean spectra. We have also shown that the difference between the empirical and theoretical models fits a general dimensional form proposed by Phillips (1988) for the contribution from breaking waves.

We have also used the theoretical model to investigate the extent to which the accuracies of wind retrievals could be affected by physical parameters that are not represented in the empirical models. Particularly important effects are swell at low incidence angles, rain at higher incidence angles, and air-sea temperature difference at low wind speeds.

The key areas for further investigation of the theoretical ocean backscatter model are summarized in the following points:

- (1) The work in this paper has focussed on comparing empirical and theoretical models of ocean backscatter at C band and Ku band in VV polarisation. The empirical models at C-VV are well developed as a result of studies with the ERS wind scatterometer. Comparisons at other frequencies and polarisations would test the theoretical modelling further. However, a previous comparison by Macklin and Stapleton (1998) of the multi-frequency model function of Unal et al. (1991) against Shuttle Imaging Radar (SIR-C) data was limited by calibration uncertainties. This points to a need for further observational data to establish more accurate multi-frequency model functions.
- (2) The performance of the theoretical model in the crosswind direction is noted as being poorer than that in the upwind direction. This suggests that the directional spread used in the wind-sea spectrum could be subject to

improvement. Additional observational data that determine the directional behaviour of the wind-sea spectrum in a consistent manner over both long and short waves are therefore desirable.

- (3) Breaking waves were identified as a possible explanation for the discrepancy between the empirical and theoretical models at large incidence angles. This explanation should be tested at other frequencies and polarisations once relevant empirical model functions are established. The directional distribution of breaking waves will differ from that of the wind sea (e.g., Phillips (1985) reports that the breaking-wave distribution is narrower by a factor of about 3), which could affect the upwind-crosswind backscatter significantly.
- (4) The theoretical model developed here is readily extended to include the effects of surface slicks (Janssen et al., 1998) and spatially varying surface currents (e.g., Romeiser and Alpers, 1997).
- (5) The theoretical models indicate that swell may have an effect on the retrieval accuracy of the wind vector. As discussed in Gommenginger et al. (2002) and Anderson et al. (2002), the estimate of significant wave height (SWH) provided by the altimeter provides additional information about the ocean surface which can be used to correct the retrieved wind speed to some extent. The off-nadir case is more complex, as the direction of swell becomes significant and information about the SWH is not directly available. One possible source of this information is a numerical wave model such as WAM, providing details of the non-local waves which can then be taken into account when retrieving local wind speed. However, the accuracy of WAM then influences the accuracy of the retrieved wind speed in a complex fashion.

Acknowledgements

This work was funded by the European Space Agency at the European Space Research and Technology Centre (ESTEC) under contract number 12934/98/NL/GD. We are grateful to the U.S. National Data Buoy Center, the Canadian Meteorological Office, and the Japanese Marine Agency for providing the buoy data used in this work.

References

- Anderson, C., Macklin, J.T., Gommenginger, C.P., and Srokosz, M.A. 2002. A comparison of the sea-state sensitivity in empirical and theoretical models of altimeter ocean backscatter. *Canadian Journal of Remote Sensing*, Vol. 28, No. 3, pp. 475–483.
- Apel, J.R. 1994. An improved model of the ocean surface wave vector spectrum and its effects on radar backscatter. *Journal of Geophysical Research*, Vol. 99, pp. 16 269 – 16 291.

- Belcher, S.E., and Vassilicos, J.C. 1997. Breaking waves and the equilibrium range of wind-wave spectra. *Journal of Fluid Mechanics*, Vol. 342, pp. 377–401.
- Bliven, L.F., Sobieski, P., and Craeye, C. 1997. Rain generated ring waves: measurements and modelling for remote sensing. *International Journal of Remote Sensing*, Vol. 18, pp. 221–228.
- Chen, K.S., Fung, A.K., and Weissman, D.E. 1992. A backscattering model for ocean surface. *IEEE Transactions on Geoscience and Remote Sensing*, Vol. GE-30, pp. 811–817.
- Colton, M.C., Plant, W.J., Keller, W.C., and Geernaert, G.L. 1995. Tower-based measurements of normalized radar cross section from Lake Ontario: evidence of wind stress dependence. *Journal of Geophysical Research*, Vol. 100, pp. 8791–8813.
- Cox, C.S., and Munk, W.H. 1954. Statistics of the sea surface derived from sun glitter. *Journal of Marine Research*, Vol. 13, pp. 198–227.
- Durden, S.L., and Vesecky, J.F. 1985. A physical radar cross-section model for a wind-driven sea with swell. *IEEE Journal of Oceanic Engineering*, Vol. OE-10, pp. 445–451.
- Elfouhaily, T., Chapron, B., Katsaros, K., and Vandemark, D. 1997. A unified directional spectrum for long and short wind-driven waves. *Journal of Geophysical Research*, Vol. 102, pp. 15 781 – 15 796.
- Freilich, M.H., and Challenor, P.G. 1994. A new approach for determining fully empirical altimeter wind speed model functions. *Journal of Geophysical Research*, Vol. 99, pp. 25 051 – 25 062.
- Geernaert, G.L., Larsen, S.E., and Hansen, F. 1987. Measurement of the wind stress, heat flux, and turbulence intensity during storm conditions over the North Sea. *Journal of Geophysical Research*, Vol. 92, pp. 13 127 – 13 139.
- Glazman, R.E. 1990. Near-nadir backscatter from a well developed sea. *Radio Science*, Vol. 25, pp. 1211–1219.
- Glazman, R.E. 1991. Statistical problems of wind-generated gravity waves arising in microwave remote sensing of surface winds. *IEEE Transactions on Geoscience and Remote Sensing*, Vol. 29, pp. 135–142.
- Goldhirsh, J. 1983. Rain cell size statistics as a function of rain rate for attenuation modelling. *IEEE Transactions on Antennas and Propagation*, Vol. AP-31, pp. 799–801.
- Goldhirsh, J., and Rowland, J.R. 1982. A tutorial assessment of atmospheric height uncertainties for high-precision satellite altimeter missions to monitor ocean currents. *IEEE Transactions on Geoscience and Remote Sensing*, Vol. GE-20, pp. 418–434.
- Gommenginger, C.P., Srokosz, M.A., Challenor, P.G., and Cotton, P.D. 2002. Development and validation of altimeter wind speed algorithms using an extended collocated buoy/Topex dataset. *IEEE Transactions on Geoscience and Remote Sensing*, Vol. 40, pp. 251–260.
- Janssen, P.A.E.M., Wallbrink, H., Calkoen, C.J., van Halsema, D., Oost, W.A., and Snoeij, P. 1998. VIERS-1 scatterometer model. *Journal of Geophysical Research*, Vol. 103, pp. 7807–7831.
- Jessup, A.T., Keller, W.C., and Melville, W.K. 1990. Measurement of sea spikes in microwave backscatter at moderate incidence. *Journal of Geophysical Research*, Vol. 95, pp. 9679–9688.
- Keller, W.C., Wismann, V., and Alpers, W. 1989. Tower-based measurements of the ocean C band radar backscattering cross section. *Journal of Geophysical Research*, Vol. 94, pp. 924–930.

- Lemaire, D., Sobieski, P., and Guissard, A. 1999. Full-range sea surface spectrum in nonfully developed state for scattering calculations. *IEEE Transactions on Geoscience and Remote Sensing*, Vol. GE-37, pp. 1038–1051.
- Long, A.E. 1995. C band and V polarized radar sea echo model from ERS-1 Haltenbanken campaign. *Journal of Electromagnetic Waves and Applications*, Vol. 9, pp. 373–391.
- Macklin, J.T., and Stapleton, N.R. 1998. Radar backscatter statistics from the sea surface: implications of SIR-C/X-SAR observations from the N.E. Atlantic. *Journal of Geophysical Research*, Vol. 103, pp. 18 827 – 18 837.
- Melsheimer, C., Alpers, W., and Gade, M. 1998. Investigation of multifrequency/multipolarization radar signatures of rain cells over the ocean using SIR-C/XC-SAR data. *Journal of Geophysical Research*, Vol. 103, pp. 18 867 – 18 884.
- Nghiem, S.V., Li, F.K., Lou, S.H., McIntosh, R.E., Carson, S.C., Carswell, J.R., Walsh, E.J., Donelan, M.A., and Drennan, W.M. 1995. Observations of radar backscatter at Ku and C bands in the presence of large waves during the Surface Waves Dynamics experiment. *IEEE Transactions on Geoscience and Remote Sensing*, Vol. GE-33, pp. 708–721.
- Nghiem, S.V., Li, F.K., and Neumann, G. 1997. The dependence of ocean backscatter at Ku-band on oceanic and atmospheric parameters. *IEEE Transactions on Geoscience and Remote Sensing*, Vol. GE-35, pp. 581–599.
- Olsen, R.L., Rogers, D.V., and Hodge, D.B. 1978. The aR^b relation in the calculation of rain attenuation. *IEEE Transactions on Antennas and Propagation*, Vol. AP-26, pp. 318–328.
- Phillips, O.M. 1985. Spectral and statistical properties of the equilibrium range in wind generated gravity waves. *Journal of Fluid Mechanics*, Vol. 156, pp. 505–531.
- Phillips, O.M. 1988. Radar returns from the sea surface — Bragg scattering and breaking waves. *Journal of Physical Oceanography*, Vol. 18, pp. 1065–1074.
- Pierson, W.J. 1991. Comment on “Effects of sea maturity on satellite altimeter measurements” by RE Glazman and SH Pilorz. *Journal of Geophysical Research*, Vol. 96, pp. 4973–4977.
- Plant, W.J. 1986. A two scale model of short wind generated waves and scatterometry. *Journal of Geophysical Research*, Vol. 91 pp. 10 735 – 10 749.
- Plant, W.J., Weissman, D.E., Keller, W.C., Hessany, V., Hayes K., and Hoppel, K.W. 1999. Air/sea momentum transfer and the microwave cross section of the sea. *Journal of Geophysical Research*, Vol. 104, pp. 11 173 – 11 191.
- Quarty, G.D., Srokosz, M.A., and Guymet, T.H. 1999. Global precipitation statistics from dual-frequency TOPEX altimetry. *Journal of Geophysical Research*, Vol. 104, pp. 31 489 – 31 516.
- Quilfen, Y., and Bentamy, A. 1994. Calibration/validation of ERS-1 scatterometer precision products. In *IGARSS '94, Proceedings of the IEEE International Geoscience and Remote Sensing Symposium*, 8–12 Aug. 1994, Pasadena, Calif. pp. 945–947.
- Romeiser, R., and Alpers, W. 1997. An improved composite surface model for the radar backscattering cross section of the ocean surface 2. Model response to surface roughness variations and radar imaging of underwater bottom topography. *Journal of Geophysical Research*, Vol. 102, pp. 25 251 – 25 267.
- Rufenach, C.L., Bates, J.J., and Tosine, S. 1998. ERS-1 scatterometer measurements — part 1: the relationship between radar cross section and buoy wind in two oceanic regions. *IEEE Transactions on Geoscience and Remote Sensing*, Vol. 36, pp. 603–622.
- Smith, S.D., Anderson, R.J., Oost, W.A., Kraan, C., Maat, N., DeCosmo, J., Katsaros, K.B., Davidson, K.L., Bumke, K., Hasse, L., and Chadwick, H.M. 1992. Sea surface wind stress and drag coefficients: the HEXOS results. *Boundary Layer Meteorology*, Vol. 60, pp. 109–142.
- Stoffelen, A., and Anderson, D.L.T. 1993. ERS-1 scatterometer data characteristics and wind retrieval skill. In *Proceedings of the 1st ERS-1 Symposium*, 1992, Cannes, France. European Space Agency, Special Publication ESA SP-359, pp. 41–47.
- Stoffelen, A., and Anderson, D. 1997. Scatterometer data interpretation: estimation and validation of the transfer function CMOD4. *Journal of Geophysical Research*, Vol. 102, pp. 5767–5780.
- Taylor, P.K., and Yelland, M.J. 2001. The dependence of sea surface roughness on the height and steepness of the waves. *Journal of Physical Oceanography*, Vol. 31, pp. 572–590.
- Unal, C.M.H., Snoeij, P., and Swart, P.J.F. 1991. The polarization-dependent relation between radar backscatter from the ocean surface and surface wind vector at frequencies between 1 and 18 GHz. *IEEE Transactions on Geoscience and Remote Sensing*, Vol. GE-29, pp. 621–626.
- Valenzuela, G.R. 1978. Theories for the interaction of electromagnetic and oceanic waves — a review. *Boundary Layer Meteorology*, Vol. 13, pp. 61–85.
- Voronovich, A.G., and Zavorotny, V.U. 2001. Theoretical model for scattering of radar signal from a rough sea surface with breaking waves. *Waves in Random Media*, Vol. 11, pp. 247–269.
- Wentz, F.J., Peteherych, S., and Thomas, L.A. 1984. A model function for ocean radar cross sections at 14.6 GHz. *Journal of Geophysical Research*, Vol. 89, pp. 3689–3704.
- Wu, J. 1991. Effects of atmospheric stability on ocean ripples: a comparison between optical and microwave measurements. *Journal of Geophysical Research*, Vol. 96, pp. 7265–7269.
- Yelland, M.J., and Taylor, P.K. 1996. Wind stress measurements from the open ocean. *Journal of Physical Oceanography*, Vol. 26, pp. 541–558.